CORRECTED PROOF

Fabrications and Na+ Storage Characteristics of Nitrogen-doped Biomass-derived Carbon Materials

Xuehu ZHANG,[a,†] Jian ZHANG,[b,c,†] Beibei HAN,[e] Kun WANG,[a,*] Guiying XU,[a,*] Yingxin WANG,[d]
Baigang AN,[a] Dongying JU,[e] Maorong CHAI,[e] and Weimin ZHOU[a,*,§] [ID]

[a] *Key Laboratory of Energy Materials and Electrochemistry Research Liaoning Province, University of Science and Technology Liaoning, Anshan 114051, China*
[b] *Hoffman Institute of Advanced Materials, Postdoctoral Innovation Practice Base, Shenzhen Polytechnic, 7098 Liuxian Blvd, Nanshan District, Shenzhen 518055, China*
[c] *School of Chemistry and Chemical Engineering, South China University of Technology, Guangzhou 510640, PR China*
[d] *JiXi Weida New Material Technology Co., Ltd., No. 8, Lexin Street, Jiguan Industrial Park, 158100, Jixi City, Heilongjiang Province, China*
[e] *Advanced Science Research Laboratory, Saitama Institute of Technology, 1690 Fusaiji, Fukaya, Japan*

* Corresponding authors: 172860635@qq.com (K. W.), xuguiying751107@163.com (G. X.), aszhou15242870697@163.com (W. Z.)

ABSTRACT

The biomass-derived carbon materials were successfully fabricated by precursor mixtures of eggplants, urea and $CaCl_2$. It is promisingly observed that controlling the mixing ratios of eggplants, urea and $CaCl_2$ can regulate the structures of fabricated carbon materials. On the basis of investigations about correlations between structures and Na+ storage capacity, it is verified that weight ratio of eggplants : urea : $CaCl_2$ = 1 : 2 : 2 is optimal to fabricate the carbon materials, which have the suitable porous structures and specific surface area to store Na+. For instance, the fabricated carbon materials show the Na+ storage capacity is 200.8 mAh/g at 0.1 A/g, after being carried out the charge-discharge 500 times. Meanwhile, the same materials also display the impressive long cycling performance. When cycling the charge-discharge 1000 times at 2.0 A/g, the fabricated carbon materials still manifest the Na+ storage capacity at 137.8 mAh/g.

1. Introduction

To face the increasingly serious energy crisis and environmental pollution, the governments in the world vigorously encourage research institutes to unfold the clean energies such as wind energy, solar energy, tidal energy and so on. Because of the clean energies manifesting the discontinuity characterization in time and space, it is difficult to make them integrated in the general power supply system.[1,2] Energy storage systems (ESSs) have just provided the ideal method to solve aforementioned anguish problems.

To date, lithium ion batteries (LIBs) and sodium-ion batteries (SIBs) have been attracted to be applied in construction of ESSs. In particular, although the SIBs show the relatively low energy density, they live up to necessary of development of ESSs in cost, for the sodium possesses the extremely abundant resources. Therefore, the studies about SIBs are becoming the hot topic exponentially in the world now.

Especially, the applicable anode materials are being studied dramatically.[3–11] It is well-known that carbon materials, titanate materials, alloy, metallic oxides and metallic sulfides are utilized as anode materials of SIBs. Thereinto, the carbon materials have extremely intrigued more than others, for they possess the some merits such as low cost, facilely fabricating, environmentally friendly and so on.

The researches regarding to the hard carbons (HCs) materials are becoming exceedingly hot topics, for their high Na+ storage capacity mainly appears at low voltage plateaus in charge-discharge processes.[12–14] In accordance with the differences of precursors, the HCs are generally classified to biomass-derived carbon and polymer-derived carbon.[15–17] In particular, the biomass-derived carbon materials are extremely attracted more than ever before, for they have prolific resource, and they are facilely fabricated. Considering the fact that eggplants which have complex pore structures are widely planted, we targeted the eggplants as carbon source to fabricate the biomass-derived carbon materials. Generally, doping N element is useful and effective way to improve the energy storage capacity of carbon materials.[18–20] $CaCl_2$ as active agent is extensively used in fabrication of activated carbon materials, for it has the obvious merits such as low cost and environmental friendliness.[21,22] Therefore, in our studies, we adopt the urea as nitrogen source and the $CaCl_2$ as active agent to fabricate biomass-derived carbon materials. As a result, the carbon materials fabricated by eggplants, $CaCl_2$ and urea in weight ratio of 1 : 2 : 2 show the fabulous storage capacity for Na+. In storage mechanism, constructing the suitable porous structures and relatively big specific surface area is pivotal factor to enhance the Na+ storage capacity.

2. Experimental

2.1 Fabrication of biomass carbons

After the eggplants had been placed in the drying oven at 100 °C to remove the water, they were ground under 74 µm. The deionized water (50 mL) was added in round bottom flask, and the eggplants, $CaCl_2$ and urea were added by weight ratios of 1 : 2 : 2, 1 : 1 : 2, 1 : 3 : 2, 1 : 2 : 1 and 1 : 2 : 3 in the same bottom flask, respectively. Thereinto, the weight of eggplants was set at 0.5 g firstly. After the obtained mixtures had been treated by ultrasonic, they were stirred at 80 °C for 2 h. The treated slurries were placed in the oven and dried at 90 °C for 12 h. The obtained solids were laid in the tube furnace and performed carbonization at 600 °C, 800 °C and 900 °C,

respectively. Continuously, the obtained carbon materials were placed in the HCl (2 M) solution and conducted the ultrasonic cleaning three times. The deionized water was used to wash the carbon materials until its pH value of washed solution became 7. Finally, the washed carbon materials were placed in the oven, and dried at 90 °C for 12 h. According to the additional amounts (weight ratio) of eggplants, CaCl$_2$ and urea, the obtained biomass-derived materials were named as ECU100, ECU122, ECU112, ECU132, ECU121 and ECU123, respectively.

2.2 Electrochemical measurements

The electrochemical cells were assembled by using the prepared composite materials. Firstly, active materials (0.08 g) mixed with acetylene black (0.01 g) and polyvinylidine fluoride (PVDF) binder (0.01 g) in a weight ratio of 80 : 10 : 10 in N-methyl-2-pyrrolidone (NMP) solution. The prepared slurry was placed on the Cu foil and dried in vacuum drying oven at 80 °C for 1 h to remove the solution. Continuously, the Cu foil with the active materials (0.9 mg/cm^2) were dried at 120 °C for 12 h in the same vacuum drying oven and cut into round shape strips of φ 11 mm in size. The cells were assembled by sodium ware in size of φ 11 mm, active materials as negative electrode and electrolyte of mixing solution of 1 M NaClO$_4$ with EC and DMC. Cyclic voltammetry (CV) and electrochemical impedance spectroscopy (EIS) measurements were carried out using the CHI 660E. The CV curves were recorded in the voltage region of 0.01–3.00 V at scan rate of 0.2 mV/s. The impedance spectra of cells (two electrodes) were tested at open circuit voltage around 2.6 V under the frequency range of 100 kHz–0.01 Hz.

3. Results and Discussion

3.1 The influence of temperature on the structures and Na$^+$ storage capacity of ECU carbon materials

It is considerable that the two factors of temperature and mixing ratio of eggplants, CaCl$_2$ and urea influence the structures of prepared biomass-derived carbons. Therefore, to inquire into the fabrication conditions in detail, we firstly maintained the mixing ratio, and mainly investigated the influence of carbonization temperature on the structures of obtained carbon materials. Thus, referring to the report,[21] we firstly adopted the mixing ratio (weight ratio) of eggplants, urea and CaCl$_2$ as 1 : 2 : 2 to prepare biomass carbons, and only investigated the influence of temperature on their structures in carbonization and activation processes. Thus, as per the changes of temperatures (600 °C, 800 °C and 900 °C) the obtained ECU1 : 2 : 2 materials were named as 600ECU122, 800ECU122 and 900ECU122, respectively.

First of all, the existence number of elements (C, N O) in ECU122 materials was investigated by element analyses and XPS measurements. As shown in Table S1, it was observed that the contents of N elements diminished with increasing the carbonization temperature, which was probably attributed to the phenomenon that the N elements as types of HCN, NH$_3$ and N$_2$ escaped from carbonization case, when increasing the carbonization temperature.[23]

The chemical states were explored by XPS measurements. The characteristic peaks of C, N and O elements were observed at 284.7 eV, 399.7 eV and 531.7 eV, respectively (Fig. 1). To further investigate the changes of chemical bonds in detail, the peak of C1s was fitted to C-C (284.6 eV), C=N&C-O (286.1 eV), C-N&C=O (287.7 eV) and O-C=O (288.8 eV), respectively. It was observed that peak about O-C=O (288.8 eV) disappeared approximately when the carbonization temperature was increased to 800 °C and 900 °C (Fig. 2).[19] Meanwhile, the peak of N1s was able to fit to the four peaks attributing to pyridinic N (397.3 eV), pyrrolic N (398.0 eV), graphite N (399.2 eV) and oxidized N (400.3 eV), respectively (Fig. S1).[24] As shown in Table S2, the contents of
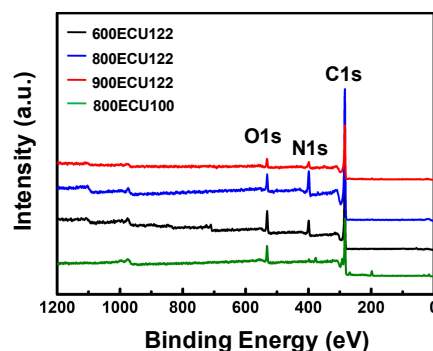

Figure 1. XPS results of ECU122 and ECU100 materials.

Pyrrolic N in 800ECU122 showed the higher percentage than that in 600ECU122 and 900ECU122. Because of Pyrrolic N having relatively high electron cloud density, it probably plays the role in enhancing the conductivity of ECU122 materials.[25]

The conversions of structure were confirmed by the XRD measurements. Compared with the carbon materials obtained by direct carbonization of eggplants, the characteristic peak at 43° disappeared in the ECU122 carbons, which presumably ascribed to the increasing of disorder in structures of ECU122 (Fig. 3).[17]

To investigate the change of microstructures of biomass carbons further, the Raman measurements were carried out in detail (Fig. S2). Similar to general carbon materials, the D peak and G peak of ECU122 and ECU100 materials were also observed at 1344 cm^{-1} and 1590 cm^{-1}, respectively. It is well-know that I_D/I_G values can reflect the structure conversions of carbon materials. Thus, it was evident that the I_D/I_G values became smaller with rising the carbonization temperature, revealing that structures of 800ECU122 and 900ECU122 became relatively order, compared with the 600ECU122 (Fig. S2).

The morphologies of 800ECU100 and 800ECU122 were described by scanning electron microscope (SEM) and transmission electron microscope (TEM) measurements. It was observed that 800ECU122 possessed the more complex porous structures than 800ECU100 (Fig. 4). In addition, the SEM-EDS results indicated that C, N and O elements homogeneously existed on the surface of 800ECU122 (Fig. S3). Furthermore, it was also observed that pseudographtic domains increased with increasing of carbonization temperature.[26] Meanwhile, the selected area electron diffraction (SAED) images of 800ECU122 and 900ECU122 showed the distinctly dispersed diffraction rings, which also was suggestive of that pseudographtic domains increased in 800ECU122 and 900ECU122 (Fig. 5).[27]

Indeed, the porous structures of ECU122 materials were evaluated by BET method. It is also obvious that the ECU122 materials exhibited the more complex structures, compared with the ECU100 materials (Fig. 6). Additionally, the 800ECU122 showed the relatively bigger specific surface area at 1023.8 m^2/g than other materials (Table S3). Meanwhile, the 800ECU122 mainly showed the pore size at 6.2 nm, which was higher than the 600ECU122 (5.0 nm), 900ECU122 (4.8 nm) and 800ECU100 (3.8 nm), respectively.

The electrochemical performances about Na$^+$ storage of ECU100 and ECU122 materials were performed via the general evaluation methods. After cycling the charge-discharge 100 times, the 800ECU122 materials exhibited the Na$^+$ storage capacity at 194.3 mAh/g, which was higher than that 600ECU122 and 900ECU122 showed the Na$^+$ storage capacity at 182.6 mAh/g and 152.0 mAh/g, respectively (Fig. 7(a)). Furthermore, the 800ECU122 still showed the Na$^+$ storage capacity at 200.8 mAh/g, while the charge-discharges were conducted 500 times. Certainly, the Na$^+$ storage
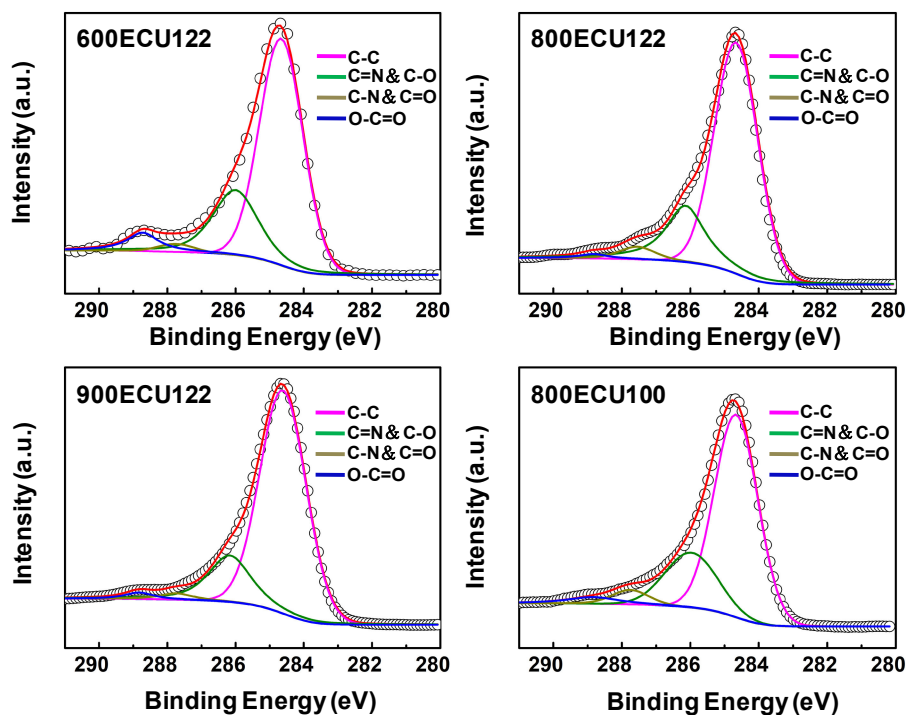
2

Figure 2. Fitting results of C1s of ECU122 and ECU100 materials.

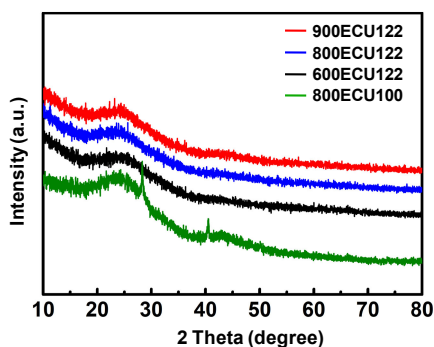**Figure 3.** XRD results of ECU122 and ECU100 materials.

Figure 4. SEM images of ECU122 and ECU100 materials.

capacity of 800ECU122 was drastically higher than the 800ECU100 showing the storage at 79.0 mAh/g. In addition, the 800ECU122 also exhibited the excellent long cycle performance. For instance, the 800ECU122 still showed Na$^+$ storage capacity at 137.8 mAh/g, after cycling the charge-discharge 1000 times at 2 A/g, which was indicative of that the 800ECU122 possessed the tremendous electrochemical stability (Fig. 7(c)).

The evaluations about rate performances were performed by continuous and different current densities such as 0.1 A/g, 0.2 A/g, 0.5 A/g, 1.0 A/g, 2.0 A/g and 5.0 A/g, respectively. After the current density was adjusted to 0.1 A/g again, the Na$^+$ storage capacity (228.2 mAh/g) of 800ECU122 was higher than the 600ECU122 (202.8 mAh/g) and 900ECU122 (139.1 mAh/g), respectively (Fig. 7(b)). These aforementioned results indicated that the 800ECU122 possessed the more fabulous rate performance than others.

The charge-discharge properties of ECU122 materials were investigated as shown in Fig. 8. Coulombic efficiencies of 600ECU122, 800ECU122 and 900ECU122 were at 26.0%, 21.8%, and 15.9% on the first cycle. Similarly, it is also considerable that the lower coulombic efficiencies are ascribed to that the ECU122 materials owned the relatively big specific surface
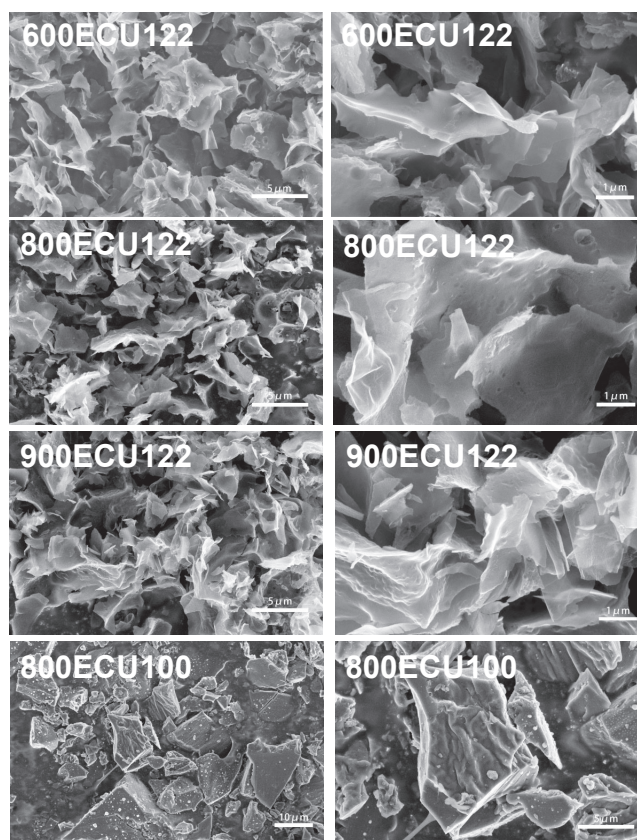
area.[18,28] Nevertheless, from second cycle, the coulombic efficiencies of 600ECU122, 800ECU122 and 900ECU122 showed an upward tendency, until the coulombic efficiencies recovered to 98%. The improvement of coulombic efficiencies was generally considered to be formation of solid electrolyte interphase (SEI) which prevents the electrolyte decomposition.

The results of electrochemical research-impedance results of ECU122 and ECU100 composite materials were described in Fig. 9. As a result, the diameter of the s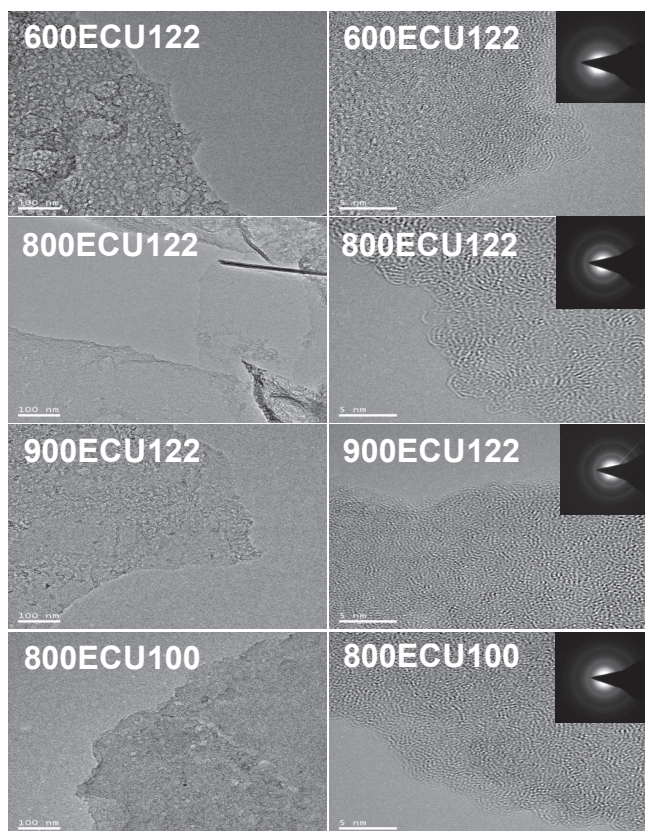emicircle of negative electrodes of 800ECU122 was much smaller than that of 600ECU122, 900ECU122 and 800ECU100, revealing that 800ECU122 possessed the impressive conductivity than other materials. Meanwhile, the impedances of 600ECU122, 800ECU122, 900ECU122 and 800ECU100 were calculated at 163.5 Ω, 84.4 Ω, 324.0 Ω and 776.5 Ω, respectively (Table S4),[29,30] which indicated that 800ECU122 owns the more excellent conductivity from another perspective.

The reason about the improvement of Na^+ storage capacity was investigated, according to the report by Wang et al.[31] As shown in Fig. 10, the capacitive contribution of 800ECU122 was calculated at 75.5 % under the sweep speed at 3 mV, which was indicative of that the capacitive effect mainly contributes to the increase of Na^+ storage capacity (Fig. 10). It is considered that cooperative effects of N-doping, suitable porous structures and big specific surface area enhance the capacitive effect. The rectangle-like behaviors of CV plots account for that the capacitive effect contributed to enhancing of storage capacity (Fig. S4).
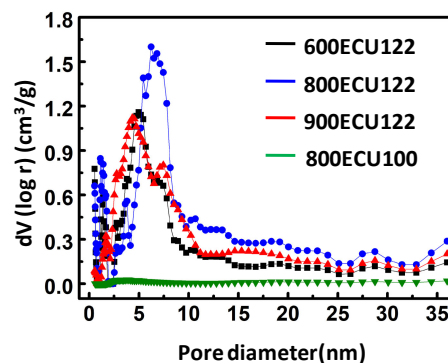

Figure 5. TEM images of ECU122 and ECU100 materials.

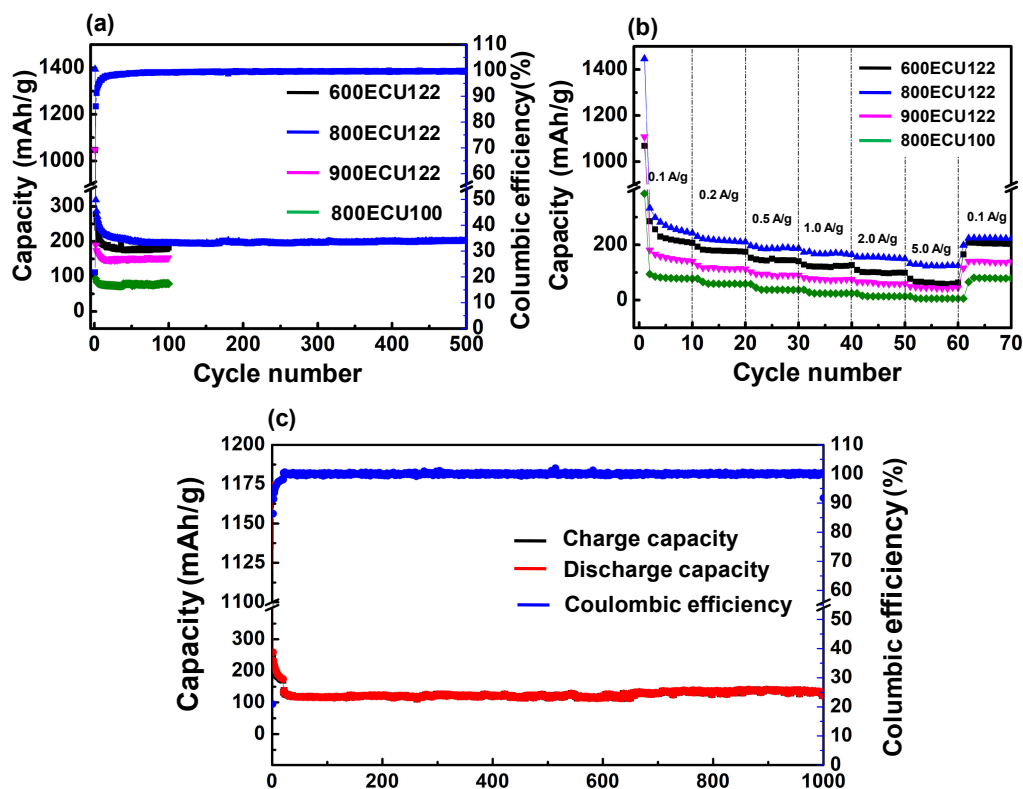**Figure 6.** Pore size distribution curves of ECU122 and ECU100 materials.

Figure 7. Cycling performances of ECU122 and ECU100 materials at current density of 0.1 A/g (a) and rate performances of ECU122 and ECU100 materials (b). (c) is the long cycling stability of 800ECU122 at 2 A/g.
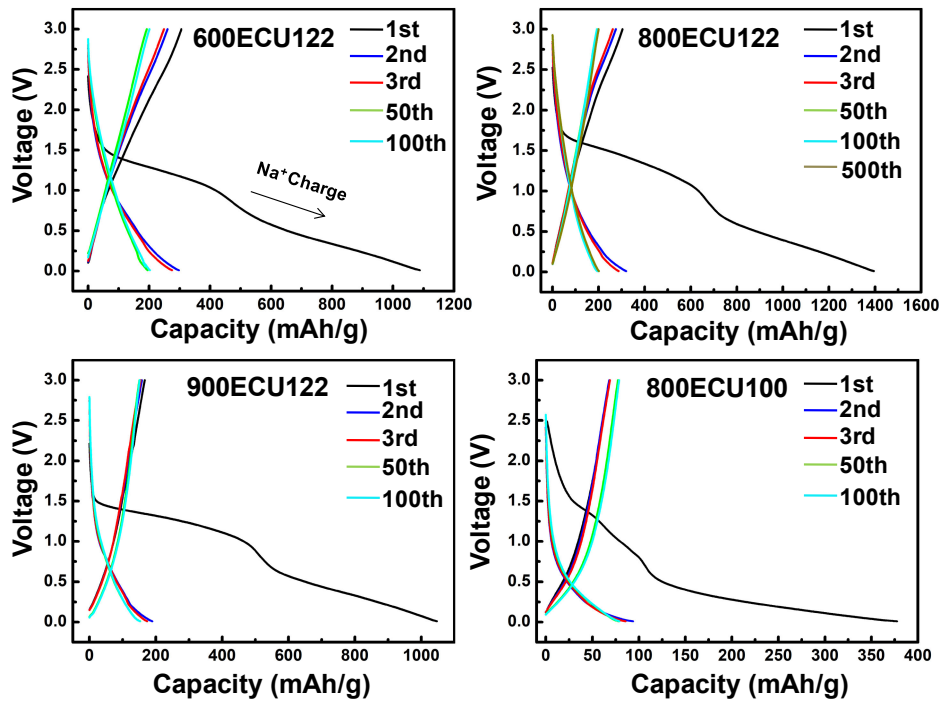
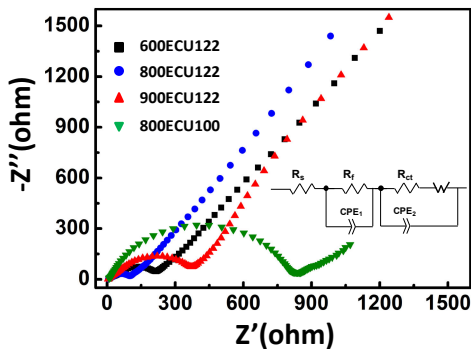**Figure 8.** Charge-discharge performances of ECU122 and ECU100 materials.

Figure 9. Nyquist plot results of ECU122 and ECU100 materials. Thereinto, the R_s, R_f, R_{ct}, CPE_1, CPE_2 and Z_W belonging to the internal resistance, equivalent circuit fitting to the plots represent the contact resistance, charge-transfer impedance, constant phase element of the SEI film, constant phase element of the electrode-electrolyte interface and Warburg impedance, respectively.
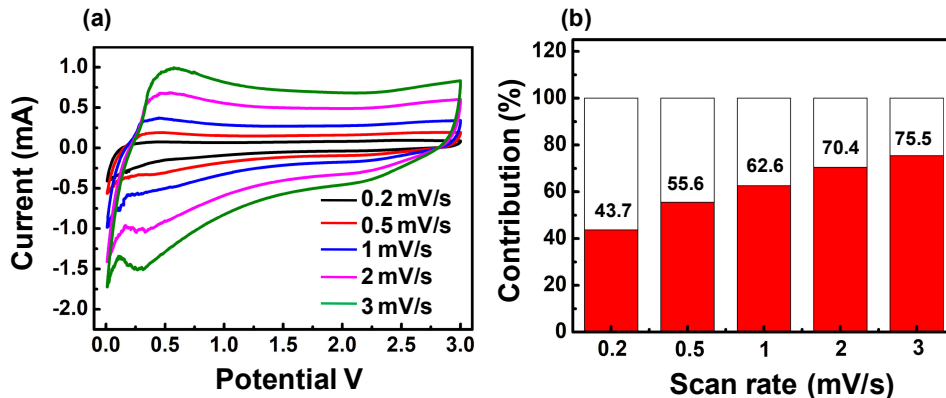
So far, associating with evaluations about Na$^+$ storage capacity, the more suitable carbonization temperature for fabrication of ECU122 carbon materials were described in detail. Continuously, the detailed investigations about the influence of each compound were carried out as following:

3.2 The influence of CaCl$_2$ content on structures and Na$^+$ storage capacity of ECU materials

The reacted ratios of eggplants, CaCl$_2$ and urea were set up at $1:1:2$ and $1:3:2$, and the carbonizations were also performed at $800\,°C$. Thus, the obtained ECU materials were named as 800ECU112 and 800ECU132, respectively. The Raman measurements were firstly used to evaluate the structural conversions of 800ECU112 and 800ECU132. Similarly, the values of I_D/I_G of 800ECU112, 800ECU122 and 800ECU132 were calculated at 2.46, 2.49 and 2.54, indicating that graphitization degree decreased with increasing the adding amount of CaCl$_2$ (Fig. S5).

Likewise, it was also observed that 800ECU112 and 800ECU132 materials possessed the complex porous structures (Fig. S6), and the sizes of pore structures were described as shown in Fig. S7. The

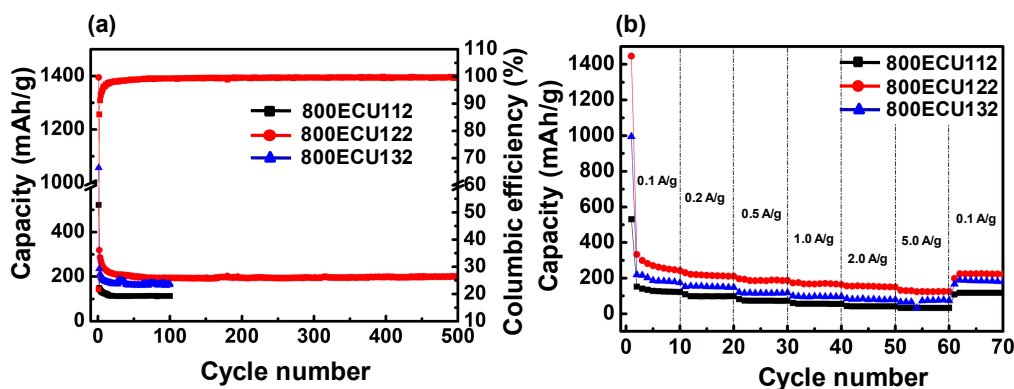**Figure 10.** Capacitive contributions for storage capacity of 800ECU122 materials. (a) shows the CV measurement results of 800ECU122 at different scan rates. (b) illustrates the bar charts showing the capacitive contribution at different scan rates.

Figure 11. Cycling performances of 800ECU112, 800ECU122 and 800ECU132 (a). (b) are the rate performances of 800ECU112, 800ECU122 and 800ECU132.
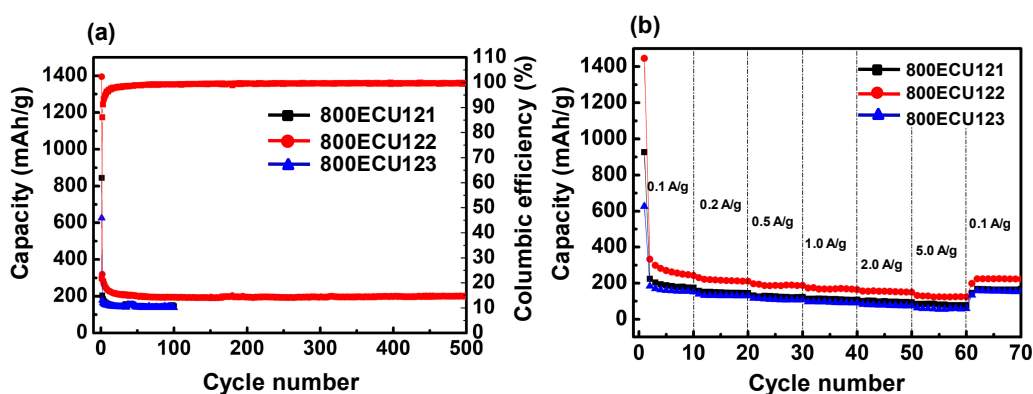

Figure 12. Cycling performances of 800ECU121, 800ECU122 and 800ECU123 (a). (b) are the rate performances of 800ECU121, 800ECU122 and 800ECU123.

800ECU112, 800ECU122 and 800ECU132 mainly showed the pore sizes at 3.0 nm, 6.2 nm and 7.5 nm respectively, revealing that pore sizes increased, while the adding amount of $CaCl_2$ was increased as well. However, the specific surface area of 800ECU132 was 754.7 m^2/g, which was smaller than the 800ECU112 (899.8 m^2/g) and 800ECU122 (1023.8 m^2/g), revealing that increasing the amount of $CaCl_2$ was limited to enlarge the specific surface area.

Likewise, the evaluations about cycling and rate performances of 800ECU112 and 800ECU132 were also performed. As shown in Fig. 11(a), after being carried out the charge-discharge 100 cycles, the 800ECU122 manifested the Na$^+$ storage at 194.3 mAh/g which was higher than the 800ECU112 (113.5 mAh/g) and 800ECU132 (159.3 mAh/g). Meanwhile, the 800ECU122 showed more excellent rate performances than 800ECU112 and 800ECU132 (Fig. 11(b)). Finally, it was obvious that 800ECU112 and 800ECU132 materials possessed the analogous charge-discharge properties with the 800ECU122, for their structures were not changed obviously (Fig. S8).

The above results indicated that the suitable $CaCl_2$ adding contents caused the suitable pore sizes and relatively big specific surface, leading to the improvement of Na$^+$ storage capacity of obtained carbon materials.

3.3 The influence of urea content on structure and Na$^+$ storage capacity of ECU materials

Furthermore, to get insight into the influence of urea on the structure and Na$^+$ storage, the reacted ratios of urea in the reactive cases of eggplants, $CaCl_2$ and urea were set up at 1 : 2 : 1 and 1 : 2 : 3. Similarly, the prepared materials were named as 800ECU121 and 800ECU123, respectively. The change of structure produced by increasing the number of N elements was investigated by Raman measurements. The I_D/I_G values of 800ECU121, 800ECU122 and 800ECU123 were calculated at 2.76, 2.49 and 3.19, respectively, indicating that 800ECU122 possessed the more excellent degree of graphitization (Fig. S9).

As shown in Fig. S10, a lot of complex porous structures also exist when changing the adding amount of urea in fabrication cases. Additionally, the calculation results by BET method revealed that 800ECU121, 800ECU122 and 800ECU123 mainly owned the pore sizes at 12.0 nm, 6.2 nm and 4.0 nm, respectively, indicating that increasing the reactive urea ratio was able to diminish the pore sizes (Fig. S11). At the same time, it was also observed that the changing of pore sizes also initiated the conversions of specific surface area. For instance, the specific surface areas of 800ECU121, 800ECU122 and 800ECU123 manifested at 725.6 m^2/g, 1023.8 m^2/g and 1148.6 m^2/g, respectively.

Likewise, the evaluations regarding to the electrochemical performances of 800ECU121, 800ECU122 and 800ECU123 were performed simply. After being performed the charge-discharge 100 cycles, the 800ECU122 exhibited the Na$^+$ storage capacity at 194.3 mAh/g, which was higher than the 800ECU121 (145.2 mAh/g) and 800ECU123 (138.2 mAh/g) (Fig. 12(a)). Additionally, the 800ECU122 also showed that more tremendous rate performances than 800ECU121 and 800ECU123 (Fig. 12(b)). Finally, it was distinct that 800ECU121 and 800ECU123 materials possessed the similar charge-discharge properties to the 800ECU122, for they owned the approximately analogous structures (Fig. S12).

CORRECTED PROOF

Although the increasing of amount of urea caused that the specific surface area became bigger than others, the narrow pore sizes lead to the fact that the 800ECU123 possessed the decreased Na^+ storage capacity. On the other side, in descriptions about influence of adding amount of $CaCl_2$, we demonstrated that increasing the adding amount of $CaCl_2$ can increase the pore sizes, but decreased the specific surface area of prepared biomass-derived carbon materials. To sum up the above analyses about the adding amounts of $CaCl_2$ and urea, it is observed that the suitable amount ratio of eggplants, $CaCl_2$ and urea is critical factor to construct suitable structures to store Na^+.

4. Conclusions

In summary, the biomass-derived carbon materials which have excellent storage performances for Na^+ were successfully fabricated by mixture of eggplants, urea and $CaCl_2$. It is found that mixing ratio by weight as 1 : 2 : 2 of eggplants, urea and $CaCl_2$ is more suitable mixing ratio to fabricate carbon materials having impressive electrochemical performances. As a result, the 800ECU122 showed Na^+ storage capacity at 200.8 mAh/g, after being carried out the charge-discharge 500 times at 0.1 A/g. Meanwhile, the 800ECU122 shows tremendous long cycling performances at 2.0 A/g. Our studies unveil that controlling the carbonization temperature and reactive ratios of carbon resource, nitrogen resource and $CaCl_2$ is able to regulate the structures of prepared carbon materials to store Na^+ ions. Considering the fact that eggplants, urea and $CaCl_2$ are facile obtainment and cheap crude materials, we think that our studies probably provide an effective and applicable way to fabricate anode materials of SIBs.

Supporting Information

The Supporting Information is available on the website at DOI: https://doi.org/10.5796/electrochemistry.21-00039.

Acknowledgments

References

1. Y. M. Li, Y. S. Hu, H. Li, L. Q. Chen, and X. J. Huang, *J. Mater. Chem. A*, **4**, 96 (2016).
2. N. Yabuuchi, K. Kubota, M. Dahbi, and S. Komaba, *Chem. Rev.*, **114**, 11636 (2014).
3. X. W. Dou, I. Hasa, D. Saurel, M. Jauregui, D. Buchholz, T. Rojo, and S. Passerini, *ChemSusChem*, **11**, 3276 (2018).
4. M. Y. Hao, N. Xiao, Y. W. Wang, H. Q. Li, Y. Zhou, C. Liu, and J. S. Qiu, *Fuel Process. Technol.*, **177**, 328 (2018).
5. M. Fukunishi, T. Horiba, M. Dahbi, K. Kubota, S. Yasuno, and S. Komaba, *Electrochemistry*, **87**, 70 (2019).
6. K. Zhang, M. Park, L. M. Zhou, G. H. Lee, J. Shin, Z. Hu, S. L. Chou, J. Chen, and Y. M. Kang, *Angew. Chem., Int. Ed. Engl.*, **55**, 12822 (2016).
7. W. J. Li, C. Han, W. L. Wang, F. Gebert, S. L. Chou, H. K. Liu, X. H. Zhang, and S. X. Dou, *Adv. Energy Mater.*, **7**, 1700274 (2017).
8. A. Karatrantos and Q. Cai, *ECS Trans.*, **72**, 11 (2016).
9. D. Wang, Z. Y. Wang, Y. Li, K. Z. Dong, J. H. Shao, S. H. Luo, Y. G. Liu, and X. W. Qi, *Appl. Surf. Sci.*, **464**, 422 (2019).
10. M. T. Lin, W. G. Yang, J. E. Hong, R. G. Oh, and K. S. Ryu, *ECS Trans.*, **59**, 27 (2014).
11. H. G. Wang, W. Li, D. P. Liu, X. L. Feng, J. Wang, X. Y. Yang, X. B. Zhang, Y. J. Zhu, and Y. Zhang, *Adv. Mater.*, **29**, 1703012 (2017).
12. D. A. Stevens and J. R. Dahn, *J. Electrochem. Soc.*, **148**, A803 (2001).
13. B. Zhang, C. M. Ghimbeu, C. Laberty, C. Vix-Guterl, and J. M. Tarascon, *Adv. Energy Mater.*, **6**, 1501588 (2016).
14. N. Sun, Z. Guan, Y. W. Liu, Y. L. Cao, Q. Z. Zhu, H. Liu, Z. X. Wang, P. Zhang, and B. Xu, *Adv. Energy Mater.*, **9**, 1901351 (2019).
15. R. R. Gaddam, D. Yang, R. Narayan, K. V. S. N. Raju, N. A. Kumar, and X. S. Zhao, *Nano Energy*, **26**, 346 (2016).
16. S. B. Wang, C. L. Xiao, Y. L. Xing, H. Z. Xu, and S. C. Zhang, *J. Mater. Chem. A*, **3**, 6742 (2015).
17. L. F. Xiao, Y. L. Cao, W. A. Henderson, M. L. Sushko, Y. Y. Shao, J. Xiao, W. Wang, M. H. Engelhard, Z. M. Nie, and J. Liu, *Nano Energy*, **19**, 279 (2016).
18. S. F. Huang, Z. P. Li, B. Wang, J. J. Zhang, Z. Q. Peng, R. J. Qi, J. Wang, and Y. F. Zhao, *Adv. Funct. Mater.*, **28**, 1706294 (2018).
19. N. Wang, Q. L. Liu, B. Y. Sun, J. J. Gu, B. X. Yu, W. Zhang, and D. Zhang, *Sci. Rep.*, **8**, 9934 (2018).
20. A. K. Radhakrishnan, S. Nair, and D. Santhanagopalan, *J. Mater. Res.*, **35**, 12 (2020).
21. J. J. Liu, R. X. Kang, Z. W. Yan, J. L. Guan, and Z. J. Quan, *Ionics*, **25**, 3907 (2019).
22. J. J. Liu, Y. F. Deng, X. H. Li, and L. F. Wang, *ACS Sustain. Chem.& Eng.*, **4**, 177 (2016).
23. Z. Y. Lin, G. Waller, Y. Liu, M. L. Liu, and C. P. Wong, *Adv. Energy Mater.*, **2**, 884 (2012).
24. X. Y. Yue, N. Huang, Z. Q. Jiang, X. N. Tian, Z. D. Wang, X. G. Hao, and Z. J. Jiang, *Carbon*, **130**, 574 (2018).
25. Q. W. Lin, J. Zhang, W. Lv, J. B. Ma, Y. B. He, F. Y. Kang, and Q. H. Yang, *Small*, **16**, 1902603 (2019).
26. S. D. Xu, Y. Zhao, S. B. Liu, X. X. Ren, L. Chen, W. J. Shi, X. M. Wang, and D. Zhang, *J. Mater. Sci.*, **53**, 12334 (2018).
27. Y. Y. Zhu, M. M. Chen, Q. Li, C. Yuan, and C. Y. Wang, *Carbon*, **129**, 695 (2018).
28. X. Zhang, C. L. Fan, and S. C. Han, *J. Mater. Sci.*, **52**, 10418 (2017).
29. X. M. Lou, C. F. Lin, Q. Luo, J. B. Zhao, B. Wang, J. B. Li, Q. Shao, X. K. Guo, N. Wang, and Z. H. Guo, *ChemElectroChem*, **4**, 3171 (2017).
30. C. F. Lin, L. Hu, C. B. Cheng, K. Sun, X. K. Guo, Q. Shao, J. B. Li, N. Wang, and Z. H. Guo, *Electrochim. Acta*, **260**, 65 (2018).
31. J. Wang, J. Polleux, J. Lim, and B. Dunn, *J. Phys. Chem. C*, **111**, 14925 (2007).